ISSN(Online): 2319-8753
ISSN (Print): 2347-6710

International Journal of Innovative Research in Science, Engineering and Technology

(An ISO 3297: 2007 Certified Organization)

Website: www.ijirset.com

Vol. 6, Issue 8, August 2017

Minimization of the DC Component in Transformerless Three-Phase Grid-Connected Photovoltaic Inverter System with Fuzzy Controller

[1] B.Leela Priyamvada [2] V.K.Chakravarthi Naik

[1]PG Scholar, Dept. of EEE, S.K.U College of Engineering & Technology, Ananthapuramu, Andhra Pradesh, India

[2]Lecturer, Dept. of EEE , S.K.U College of Engineering & Technology, Ananthapuramu, Andhra Pradesh, India.

ABSTRACT: In the power systems the dc component can affect the operating point of the transformers. The transformer cores are determined into unidirectional saturation with consequent larger excitation current. The transformer reduces the inrush currents and maintains required voltages but for low frequency (50 or 60 HZ) transformer is bulky, heavy, and expensive so its power loss brings down the overall system efficiency. Then the PV array is connected to the grid via a two level inverterthree phase voltage source and an LCL filter is replaced instead of the transformer. The edge for dc module in the grid side ac currents is below 0.5% of the rated current. The dc component can cause dc-link voltage ripple, line frequency power ripple and further second order harmonic in an ac current. To reduce the dc component in three phase ac currents the real solution is shown in this paper is to mimic the blocking capacitors used for the dc component reductionis called as virtual capacitor. The “virtual capacitor” is attained by adding an integral of the dc module in the current response path. The accurate extraction of the dc component can achieve the control, harmonic conditions and approved effective even under grid frequency variation. A proportional integral resonant controller is additional designed to regulate the dc and line frequency module in the current loop to deliveraccurate control of the dc current.Here fuzzy logic is used for controlling compared to other controllers. The Simpered Systems tool has demonstrated that the joint system will at the same time inject maximum power from a PV unit and compensate the harmonic current drained by nonlinear loads.

I. LITERATURE REVIEW ANDRELATED WORKS

The elimination of the output transformer from grid- connected photovoltaic (PV) systems not only reduces the cost, size, and weight of the conversion stage but also increases the system overall efficiency.
However, if the transformer is removed, the
Galvanic isolation between the PV generator and the grid is lost. This may cause safety hazards in the event of ground faults. Various inverter topologies are presented, compared, and evaluated against demands, lifetime, component ratings, and cost. Finally, some of the topologies are pointed out as the best candidates for either single PV module or multiple PV module applications[1]. The accuracy of the DC current sensor then becomes important to achieving this. A scheme is proposed in which DC link current sensing and current control are used to minimize the output DC current component. Current
Controllers are affected by errors associated
resistance of the distribution grid conductors, canceling the DC voltage component at the Point of Common Coupling (PCC) implies the compensation of the DC current injection by electric loads or grid connected converters connected at the same PCC [5]. The main goal is to ensurea reduction of the switching frequency ripple at a reasonable cost and, at the same time. The experimental results demonstrate the effectiveness of the design procedure both of the LCL-filter and of the controllers. The performance of the overall system is good both in the low and high frequency ranges [3].

ISSN(Online): 2319-8753
ISSN (Print): 2347-6710

International Journal of Innovative Research in Science, Engineering and Technology

(An ISO 3297: 2007 Certified Organization)

Website: www.ijirset.com

Vol. 6, Issue 8, August 2017

II. EXISTING SYSTEM

There are many problems related to transformerless structures, like dc element within the electrical converter output (grid) current, ground run current (due to common-mode voltage and parasitic capacitance), and also the voltage-level mate between the electrical device (inverter) and grid. Among them, the dc element will have an effect on the normal system operation and cause safety issues. Standards have so been established in several countries to limit the extent of the dc element.

Disadvantages of Existing System

The dc component can have negative impacts on the power system in the following ways :

1) The dc component can affect the operating point of the transformers in the power system. The transformer cores are driven into unidirectional saturation with consequent larger excitation current. The service lifetime of the trans-former is reduced as a result with further increased hysteresis and eddy current losses and noise.

2) The dc component can circulate between inverter phase legs as well as among inverters in a paralleled configuration. The dc component circulation affects the even current and loss distribution among paralleled inverters.

3) The dc component injected to the grid can affect the nor-mal operation of the loads connected to the grid, for example, causing torque ripple and extra loss in ac motors.

4) The corrosion of grounding wire in substations is intensified due to the dc component.

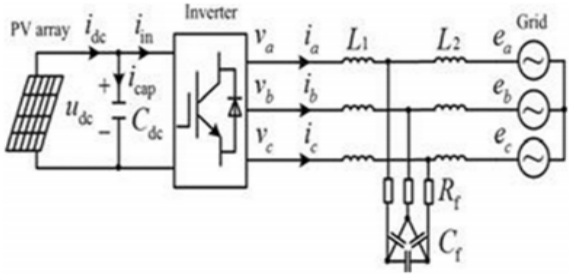

Fig 1: Transformerless three-phase PV inverter system.

In the proposed control plan, an exact dc component quantity and extraction is critical. Here several devices can be used to amount the dc module, e.g., by shunt resistors, voltage transformers, mutual coupled inductors, and integral methods, etc. Among them, only the integral methods do not need additional hardware. So a new integral method based on the sliding window double time and iteration algorithm integral is presented. This technique is active in the extraction of the dc module even for currents with frequency fluctuations and harmonics.

III.IMPACT OF THE DC COMPONENTS ON PV SYSTEMS

A typical three phase transformer less PV inverter system is shown in Fig. 1. The PV array is connected to the grid via three phase voltage source two level inverter and an LCL filter. The capacitors of the LCL filter are configured with a delta or star connection. In this paper, to reduce the required capacitor and cost a deltaconnection is used as opposed to the star connection, which has the benefitof smaller short-circuit current. The dual closed loop control strategy comprises a current and a dc-link voltage loop in the synchronous rotational frame, is a common control strategy in three phase PV inverters.

$$\begin{cases} Fa = Fa0 + Fa1 \\ Fb = Fb0 + Fb1, \\ Fc = Fc0 + Fc1 \end{cases} \begin{cases} F\alpha = F\alpha 0 + F\alpha 1 \\ F\beta = F\beta 0 + F\beta 1 \end{cases}, \begin{cases} Fd = Fd0 + Fd1 \\ Fq = Fq0 + Fq1 \end{cases}$$

_____ (1)

Wherethe subscript 0 denotes the dc component and the subscript 1 denotes the line-frequency component. If there are dc components in the abc coordinate, they will also exist in the form of dc or line-frequency components in αβ and dq

ISSN(Online): 2319-8753
ISSN (Print): 2347-6710

International Journal of Innovative Research in Science, Engineering and Technology

(An ISO 3297: 2007 Certified Organization)

Website: www.ijirset.com

Vol. 6, Issue 8, August 2017

coordinates, respectively. In a three-phase three-wire system, there is no current flowing through the neutral point and hence the line frequency is

$$\begin{cases} Fa0 = Fb0 + Fc0 = 0 \\ Fa1 = Fb1 + Fc1 = 0. \end{cases} \quad \text{_____ (2)}$$

With (1) and (2), the coordinate transformations of the dc components from abc coordinate to αβ and dq coordinate can be expressed as

$$\begin{pmatrix} F\alpha 0 \\ F\beta 0 \end{pmatrix} = \frac{2}{3}\begin{pmatrix} 1 & -\frac{1}{2} & -\frac{1}{2} \\ 0 & \frac{\sqrt{3}}{2} & -\sqrt{3}/2 \end{pmatrix} \cdot \begin{pmatrix} Fa0 \\ Fb0 \\ Fc0 \end{pmatrix} = \begin{pmatrix} Fa0 \\ \frac{\sqrt{3}}{3Fb0} - \sqrt{3}/3Fco \end{pmatrix}$$

_____ (3)

$$\begin{pmatrix} Fd1 \\ Fq1 \end{pmatrix} = \frac{2}{3}\begin{pmatrix} \cos\theta & \sin\theta \\ -\sin\theta & \cos\theta \end{pmatrix} \cdot \begin{pmatrix} 1 & -\frac{1}{2} & -\frac{1}{2} \\ 0 & \frac{\sqrt{3}}{2} & -\frac{\sqrt{3}}{2} \end{pmatrix} *$$

$$\begin{pmatrix} Fa0 \\ Fb0 \\ Fc0 \end{pmatrix} = \begin{pmatrix} Fa0\cos\theta + \frac{\sqrt{3}}{3}[Fa0 - Fco]\sin\theta \\ \frac{\sqrt{3}}{3}[Fb0 - Fco]\cos\theta - Fa0\sin\theta \end{pmatrix}$$

_____ (4)

Where θ is the angle between the dqcoordinate and abc coordinate for example, the grid angle in a grid voltage oriented vector control.

Asin (3) and (4) the coordinate transformation, F_{a0}, F_{b0} and F_{c0}(dc components) in the stationary abc frame can be transformed into $F_{\alpha 0}$ and $F_{\beta 0}$in the stationary αβ frame and then $F_{d1}$and F_{q1}(line frequency) in dq frame.

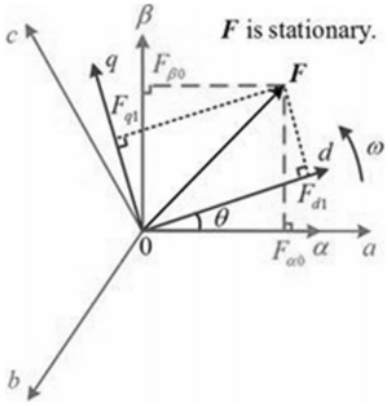

Fig 2: Coordinate transformation of dc components.

ISSN(Online): 2319-8753
ISSN (Print): 2347-6710

International Journal of Innovative Research in Science, Engineering and Technology

(An ISO 3297: 2007 Certified Organization)

Website: www.ijirset.com

Vol. 6, Issue 8, August 2017

$$P_{ac} = 3/2\begin{bmatrix} Ud \\ Uq \end{bmatrix} T.\begin{bmatrix} Id \\ Iq \end{bmatrix} = 3/2\begin{bmatrix} ud0 + ud1 \\ uq0 + uq1 \end{bmatrix} T.\begin{bmatrix} id0 + id1 \\ iq0 + iq1 \end{bmatrix}$$

$$= \frac{3}{2}\begin{bmatrix} ud0id0 + q0iq0 + \\ DC\ component \\ +ud0id1 + ud1id0 + uq0iq1 + uq1iq0 + \\ Line - frequency\ fluctuation \\ ud1id1 + uq1i1 \\ 2nd\ fluctuation \end{bmatrix}$$

_____ (5)

$$q_{ac} = 3/2\left\|\begin{bmatrix} Ud \\ Uq \end{bmatrix} T*\begin{bmatrix} Id \\ Iq \end{bmatrix}\right\| = 3/2\left\|\begin{bmatrix} ud0 + ud1 \\ uq0 + uq1 \end{bmatrix} T*\begin{bmatrix} id0 + id1 \\ iq0 + iq1 \end{bmatrix}\right\| \text{ (T = transpose)}$$

$$= \frac{3}{2}\begin{bmatrix} ud0id0 + q0iq0 + \\ DC\ COMPONENT \\ +ud0id1 + ud1id0 + uq0iq1 + uq1iq0 + \\ LINE - FREQUENCY\ FLUCTUATION \\ ud1id1 + uq1iq1 \\ 2nd\ FLUCTUATION \end{bmatrix}$$

_____ (6)

As shown, both the active and reactive power contains a line frequency, aconstant dc power and a second order power fluctuation due to the dc component in the currentand voltage undesired. Further, with grid voltage orientated vector control under unity power factor operation for PV applications, where $u_{q0}=0$, $i_{q0}=0$, (5) and (6) can be simplified as (7) and (8) if assuming the second order fluctuations is negligible compared to the other two components.

$$p_{ac} = \frac{3}{2}\begin{pmatrix} ud0id0 \\ DC\ component \\ +ud0id1 + ud1id0 \\ Line - frequency\ fluctuation \end{pmatrix}$$

_____ (7)

$$q_{ac} = \begin{pmatrix} uq1id0 - ud0iq1 \\ Line - frequency\ fluctuation \end{pmatrix}$$

_____ (8)

ISSN(Online): 2319-8753
ISSN (Print): 2347-6710

International Journal of Innovative Research in Science, Engineering and Technology

(An ISO 3297: 2007 Certified Organization)

Website: www.ijirset.com

Vol. 6, Issue 8, August 2017

IV.PROPOSED TECHNOLOGY

A.Virtual capacitor concept of a single-phase grid-connected PV inverter

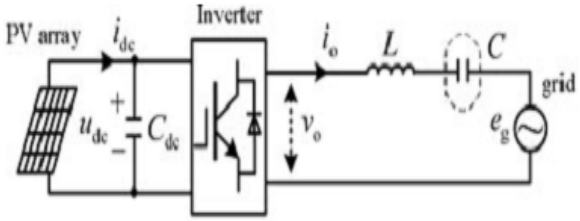

(a) Circuit diagram of a single-phase grid-connected PV inverter with the blocking capacitor.

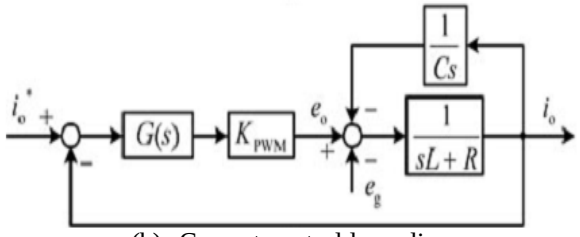

(b) Current control loop diagram.

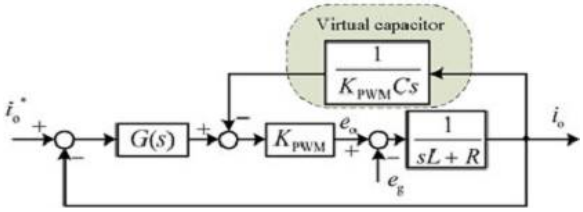

(c) Equivalent transformation of the current control loop with virtual capacitor concept.

Fig 3: Virtual capacitor concept of a single-phase grid-connected PV inverter.

To block the dc component put a capacitor Cin series with the ac side of the inverter shown in Fig. 3(a). However, in order to reduce the capacitive reactance at other frequencies, the value of the capacitor must be large; it increases the size and cost of the system. This series capacitor may also disturb the system dynamic response and reduce transmission efficiency. However, the physical capacitor is replaced by software based method and advanced control strategy mimics the operation of the series capacitor in a single phase PV system.

$$L\,(di0/dt) + 1/C\int i0dt + Ri0 = eg - v0 \quad \text{..... (9)}$$

$$I_0(s) = \frac{Cs}{LCs2 + RCs + 1}\left[E_g(s) - V_0(s)\right] \quad \text{..... (10)}$$

Where v_0 and $i_0$are the inverter output voltage and current, respectively; e_g is the gird voltage; Vo(s), Io(s), and Eg(s) are the Laplace transforms of v_0, i_0, and e_g in the frequency domain, respectively;Lis the filter inductance; Ris the line equivalent resistance; and Cis the blocking capacitor. Substituting the operatorsin (10) withjω,Io(jω) equals zero when ω=0(dc). This indicates that the blocking capacitor can minimize the dc component effectively.

ISSN(Online): 2319-8753
ISSN (Print): 2347-6710

International Journal of Innovative Research in Science, Engineering and Technology

(An ISO 3297: 2007 Certified Organization)

Website: www.ijirset.com

Vol. 6, Issue 8, August 2017

B. Virtual capacitor implementation for a three-phase PV inverter

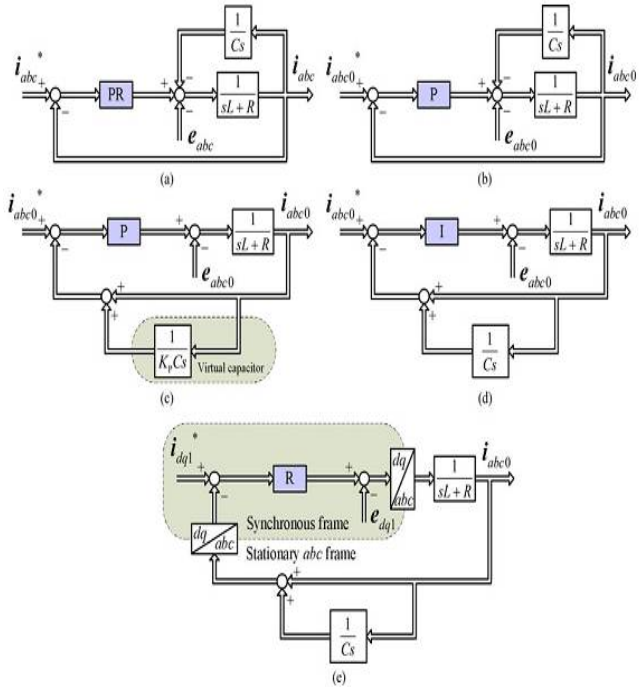

Fig 4: Virtual capacitor implementation for a three-phase grid-connected PV inverter: (a) current control loop in stationary a-b-c frame, (b) dc component control loop in stationary a-b-c frame, (c) equivalent transformation of the dc component control loop with virtual capacitor, (d) dc component control loop based on an integral(I) controller, and (e) dc component control loop in a mixed frame (d-q and a-b-c).

C. Mathematical model of the three-phase PV inverter with blocking capacitors in the Synchronous frame

Based on the virtual capacitor concept in the single phase system aims to derive the three phase system models with blocking capacitors in different frame and inspect the correctness of applying the virtual capacitor concept to three-phase systems in each frame. Fig. 5 shows the circuit diagram of a three-phase PV inverter with blocking capacitors (C).

$$Ldi_a/dt + 1/C\int = e_a\text{-}v_a$$
$$Ldi_b/dt + 1/C\int = e_b\text{-}v_b$$
$$Ldi_c/dt + 1/C\int = e_c\text{-}v_c \quad \text{_____ (11)}$$

Where L is the equivalent inductance which includes Inverterside inductance L1 and the grid side inductance L2.The definitions of other variables in (11) are denoted in fig (5). Especially v_a, v_b and v_c are the average values of inverter side voltage over a switching period. Note that the inverter duty cycle I not included in the average model in (11) to simplify the control design. A more rigorous invertor small signal model can be founding.

$$\begin{cases} \dfrac{Ldi\alpha}{dt} + 1/C\int i\alpha dt + Ria = e\alpha - v\alpha \\ \dfrac{Ldi\beta}{dt} + \dfrac{1}{c}\int i\beta dt + Ri\beta = e\beta - v\beta \end{cases} \quad \text{___ (12)}$$

In order to further derive the models in frequency domain on the synchronous rotational dq frame, complex vectors are synthesized from scalars in ±² and dq frame as shown

ISSN(Online): 2319-8753
ISSN (Print): 2347-6710

International Journal of Innovative Research in Science, Engineering and Technology

(An ISO 3297: 2007 Certified Organization)

Website: www.ijirset.com

Vol. 6, Issue 8, August 2017

$$\begin{cases} f\alpha\beta = f\alpha + jf\beta \\ fdq = fd + jfq \end{cases} \quad \text{_____ (13)}$$

Where f is general complex vector which can representsvoltage and current. With the complex vector expression in (13), the system model in α-β.

Frame in (12) can be transformed to the complex vector form as given in

$$L(di\alpha\beta/dt+1\int i\alpha\beta dt + Ri\beta = e\alpha\beta - v\alpha\beta \quad \text{_ (14)}$$

$$I_{\alpha\beta}(s) = \frac{Cs}{LCs2 + RCs + 1}\,[E_{\alpha\beta}(s) - V_{\alpha\beta}(s)] \quad \text{_____ (15)}$$

$$Idq(s) = \frac{C[s + jw]}{Ls[s + jw]2 + RC[s + jw] + 1} * [Edq(s) - Vdq(s)] \quad \text{_____ (16)}$$

Substituting (13) in (16), the mathematical model for the three phase system with blocking capacitors in dq frame can be derived as

$$\begin{aligned} \{Id(s)\,LCs\,2 + RCs - Lw2 + 1] - Iq(s)\,[2LSws + RCw\} &= \\ [Ed\,(s) - Vd(s)]\,Cs - [Eq(s) - Vq(s)] & \\ Cw.Id(s)\,[2LCws + RCw] + Fq(s)\,[LCs2 + RCs - LCw2 + 1] &= \\ Ed(s) - Vd(s)]Cw + Eq(s) - Vq(s)]\,Cs & \end{aligned} \quad \text{_____ (17)}$$

Shown in (17), after adding blocking capacitors to the ac side of the power circuit, there are strong couplings between the d and q axis is very difficult to be decoupled. This specifies that the virtual capacitor should not be in the standard synchronous rotational dq frame but in the stationary abc frame.

D. DC component minimization in three-phase PV inverters with DC-Component Feed-Forward and PIR Controller

Based on the above analysis, this section investigates how to implement the "virtual capacitor" concept for three phase systems in the stationary frame and to be further integrated to the standard PV inverter current control loop in the dq frame with a PIR controller. The standard three phase inverter loopnormally adopts a proportional integral (PI) controller to regulate the d-axis and q-axis currents.

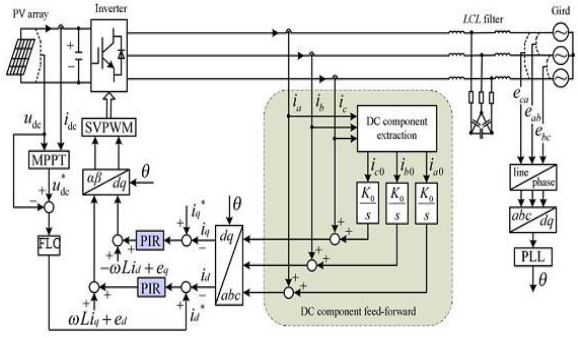

Fig 5: DC component minimization strategy based on dc component feed-forward and PIR-controller.

ISSN(Online): 2319-8753
ISSN (Print): 2347-6710

International Journal of Innovative Research in Science, Engineering and Technology

(An ISO 3297: 2007 Certified Organization)

Website: www.ijirset.com

Vol. 6, Issue 8, August 2017

The PI controller in dq frame is equivalent to a proportional-resonant (PR) controller in the stationary abc frame given the resonant frequency of the R controller andselected as the line rotational frequency. Therefore, the current control loop of three phase inverters with blocking capacitors in stationary abc frame can be represented as shown in Fig. 4(a), where the variables of subscript abcdenote the vectors of the three phase voltages and currents. The gain of the pulse width modulator (KPWM) is assumed to be unity to simplify the derivation.

V.DC COMPONENT EXTRACTION BASED ON SLIDING WINDOW ITERATION

In the control strategy shown in Fig. 5, an accurate dc component measurement and extraction is the key to implement the virtual capacitor concept and achieve the overall dc component minimization.

As mentioned, the dccomponent needs to be reduced within 0.5% of the rated output current. Compared with the ac component, the dc component is very small and an accurate dc component extraction is stimulating. In PV inverters, the Hall Effect current sensors are widely used to measure the ac side currents (including both ac and dc components) due tothesmallersize, isolated output, and wide bandwidth (e.g., from dc to several hundred kilohertz). An integral method based on the sliding window iteration algorithmis used in this paper to extract the dc component from the ac side currents.

Taking the ac side Phase A current $i_a$can be expressed in (18) if considering both the dc component and other ac components of different frequencies (e.g., harmonics).

$$ia = ia0 = \sum_{h=1,2,3}^{n} \sin\left[2\pi f1t + \psi h\right] \quad \text{(18)}$$

Where i_{a0} is the dc component, f_1 is the line frequency. I_h, hf_1, and $\Psi_h$are the amplitude, frequency, and phase angle of the fundamental and harmonic components. Averaging the integration of (18) in the interval from $t_0$tot$_0$+T yields

$$\frac{1}{T}\int_{t0}^{t0+T} iodt = 1/T\left[\int_{t0}^{t0+T} ia0dt + \int_{t0}^{t0+T} \sum_{h=1,2,3,..} In\sin\left[2\pi f1t + \varphi hdt\right]\right] \quad \text{(19)}$$

When T = T_1= 1/f_1, the second term in the right side of (19) becomes $\int_{t0}^{t0+T} \sum_{h=1,2,3,.....} Ih\sin\left[2\pi f1t + \varphi h\right]dt = 0$ (20)

Hence the (19) and (20) of dc component i_{a0}can be obtained by

$$ia0 = \frac{1}{T1}\int_{t0}^{t0+T} iadt \quad \text{(21)}$$

The next step is to implement the expression in (21) toobtain the dc component ia0 accurately without significant calculation burden. If assuming the number of sampling times in a fundamental period (T_1) is N, dt in (21) can be substituted by the sampling interval Δt and Δt =T1/N. If τ is defined as t/N, then Ia (kτ) is the kth sampling value. Substituting the definiteintegration in (21) by the accumulation of the integrand, the discrete expression of i_{a0} is given by

$$ia0 = \frac{1}{N\Delta T}\sum_{k=0} ia\left(KT\right)\Delta t = \frac{1}{N}\sum_{k=0}^{N-1} ia\left(KT\right) \quad \text{(22)}$$

To achieve a real time dc component extraction the sampling values for N_1timesinone fundamental period is therefore significant given a high sampling frequency. To decrease the amount of calculation, sliding window iteration is used in (23) to replace (22)

$$ia0 = \frac{1}{N}\sum_{k=Ncut-N+1}^{Ncut} i0\left(KT\right) = \frac{1}{N}\sum_{k=Ncut-N}^{Ncut-1} ia\left(KT\right) - ia\left(Ncut - NT\right) + ia\left(NcutT\right) \quad \text{(23)}$$

Where $N_{cur}$is sliding pointer represent the current sampling point. After completing the summation of one fundamental period for initialization, N–1 additions of (22) is simplified as one addition and one subtraction of (23). As a result, the amount is reduced. The dc component calculation method based on the sliding window iteration is illustrated in Fig. 6.

ISSN(Online): 2319-8753
ISSN (Print): 2347-6710

International Journal of Innovative Research in Science, Engineering and Technology

(An ISO 3297: 2007 Certified Organization)

Website: www.ijirset.com

Vol. 6, Issue 8, August 2017

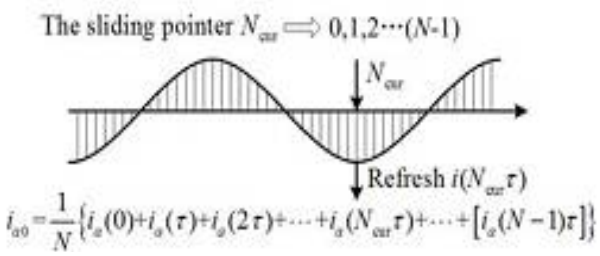

Fig 6: Diagram of the dc component calculation based on sliding window iteration.

Which contains a dc component (step signal at 0.08 s), f_1= 49 .5Hz, fifth and seventh order harmonics

$$ia = 0.5\varepsilon(t-0.08) + 10\sin(2\pi f1t) + 1.5\sin(10\pi f1t) + 0.5\sin(14\pi f1t) \quad (24)$$

The dc component extraction method is implemented and tested in MATLAB/Simulink. Here the fuzzy controller is used compared to alternative controllers because of its accurate performance.

VI.PIR CONTROLLER DESIGN

As mentioned, when taking the dc component in the ac-side currents into account, the current loop in the dq frame is composed of both a dc component and a line-frequency component (negative sequence). The dc component in the rotational frame comes from the line-frequency ac components in the phase currents.

From the dc component the phase currents provide an effective control for both dc and line frequency signals in the dq frame and a proportional integral resonant (PIR) controller is used.

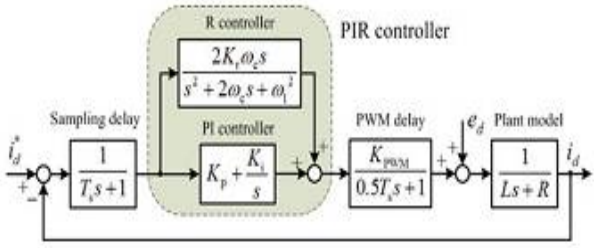

Fig 7: d-axis current loop based on the PIR controller.

Taking the d-axiscurrent control loop the sampling delay and the PWM delay, the current control loop based on the PIR controller is shown in Fig. 7.

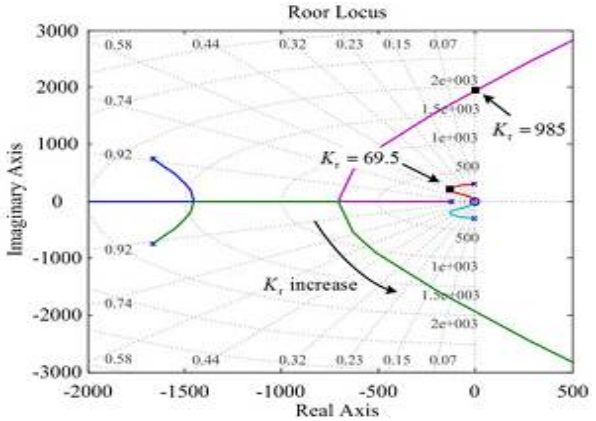

Fig 8: Root locus of the current loop with K_r varying from 0 to infinite.

ISSN(Online): 2319-8753
ISSN (Print): 2347-6710

International Journal of Innovative Research in Science, Engineering and Technology

(An ISO 3297: 2007 Certified Organization)

Website: www.ijirset.com

Vol. 6, Issue 8, August 2017

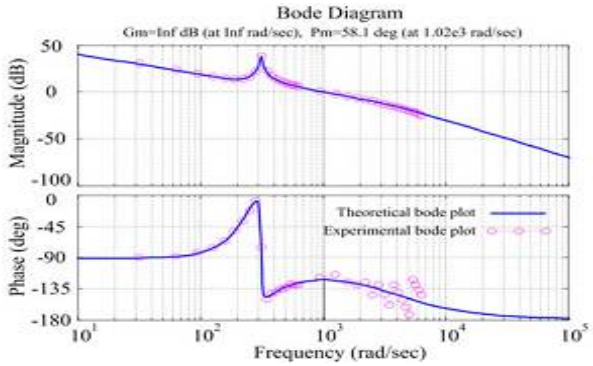

Fig 9: Theoretical open-loop bode plot of the current loop with a PIR controller for L=2.7mH, R=0.3Ω, ω_c= 5rad/s, Kp=2.7, Ki=300, and Kr=69 .5.

As expected, the bode plot has both high gain at dc and line frequency. The phase margins (Pm = 58.1°) indicates that the designed current loop is stable.The system is simulated in MATLAB/Simpered Systems and Fuzzy simulated system is shown in fig.10 to the accurate extraction of the dc component can achieve the control, harmonic conditions and approved effective even under grid frequency variation.

VII.FUZZY LOGIC CONTROL

The Fuzzy logic control consists of set of linguistic variables. Here the PI controller is replaced with Fuzzy Logic Control. The mathematical modeling is not required in FLC. FLC consists of

i)Fuzzification

Membership function values are assigned to linguistic variables. In this scaling factor is between 1 and -1.

ii)Inference Method

There are several composition methods such as Max-Min and Max-Dot have been proposed and Min method is used.

iii)Defuzzification

A plant requires non fuzzy values to control, so defuzzification is used. The output of FLC controls the switch in the inverter. To control these parameters they are sensed and compared with the reference values. To obtain this the membership functions of fuzzy controller are shown in fig (7).

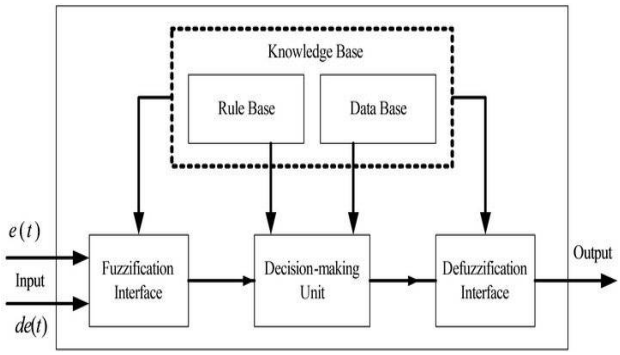

Fig 10: Fuzzy Logic Controller.

The set of FC rules are derived from

u=-[α E + (1-α)*C]_____ (25)

ISSN(Online): 2319-8753
ISSN (Print): 2347-6710

International Journal of Innovative Research in Science, Engineering and Technology

(An ISO 3297: 2007 Certified Organization)

Website: www.ijirset.com

Vol. 6, Issue 8, August 2017

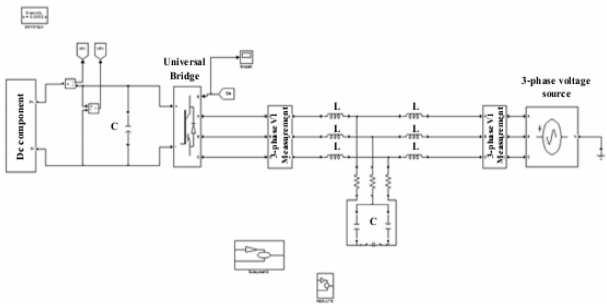

Fig 11: Simulation system schematic diagram.

VIII.SIMULATION RESULTS

The dc component extraction method is implemented and tested in MATLAB/Simulink. Here the fuzzy controller is used compared to alternative controllers because of its accurate performance. Simulation results of the dc component extraction method under frequency deviation and with harmonics are shown in Fig. 12. Fig. 12 shows the measured ac side current signal which contains fifth and seventh harmonics as well as a dc component appearing from 0.08 s. Fig. 13 shows the dc component in the current signalwithamplitudeof 0.5A. Fig.14shows the simulation results of the dc component extraction method.As seen, although the average value of the dc component is estimated correctly as 0.5A, line frequency fluctuation exists in i_{a0}because of the frequency deviation.

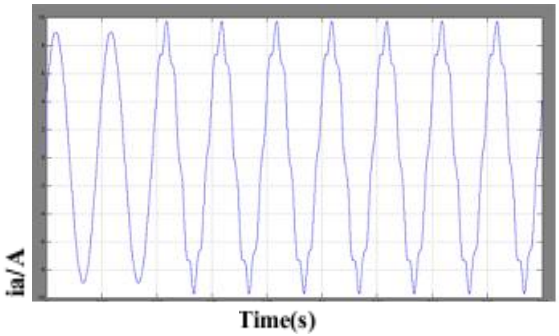

Fig 12: Grid current waveforms with dc component.

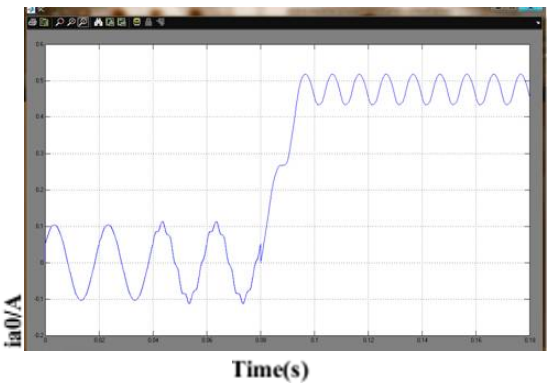

Fig 13: Minimized dc component of Grid current waveforms by single integral.

ISSN(Online): 2319-8753
ISSN (Print): 2347-6710

International Journal of Innovative Research in Science, Engineering and Technology

(An ISO 3297: 2007 Certified Organization)

Website: www.ijirset.com

Vol. 6, Issue 8, August 2017

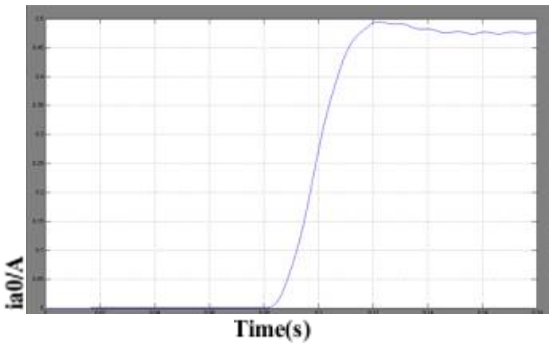

Fig 14: Minimized dc component of Grid current waveforms by double integral.

Extension results with FLC

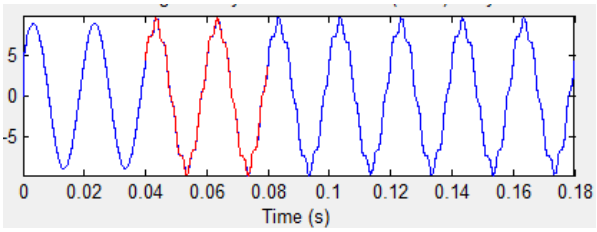

Fig 15: Measured phase A (grid) current.

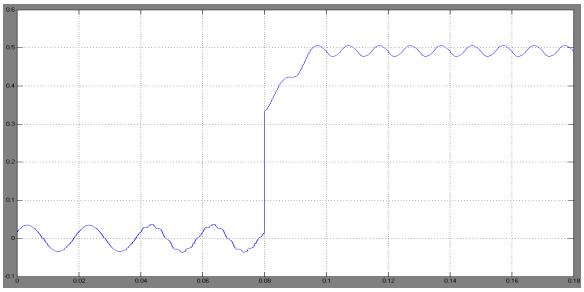

Fig 16: Minimized dc component of Grid current waveforms by single integral with fuzzy controller.

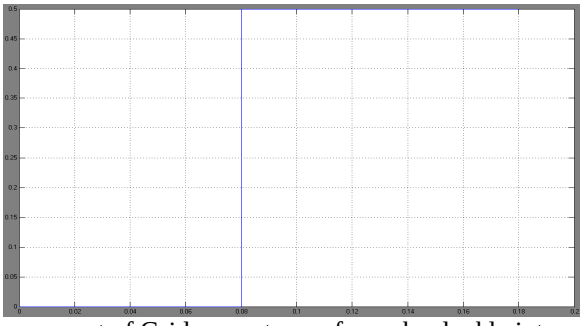

Fig 17: Minimized dc component of Grid current waveforms by double integral with fuzzy controller.

ISSN(Online): 2319-8753
ISSN (Print): 2347-6710

International Journal of Innovative Research in Science, Engineering and Technology

(An ISO 3297: 2007 Certified Organization)

Website: www.ijirset.com

Vol. 6, Issue 8, August 2017

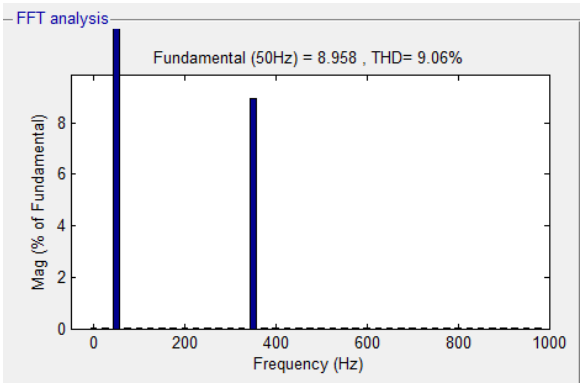

Fig 18: THD value of transformerless three-phase grid-connected PV inverter.

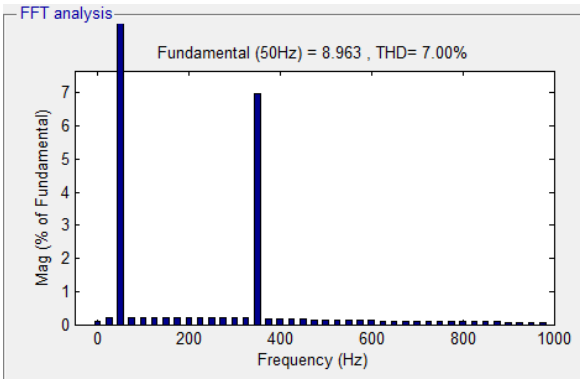

Fig 19: THD value with fuzzy controller.

However, compared to the original current $i_a$in Fig. 12, the ac components have been attenuated effectively. To further eliminate the ripple on the extracted dc component in Fig. 13, with which the ripple can be effectively attenuated, and the result is shown in Fig. 14.As seen, the exact dc component can accurately reflect the original dc signal after a short transition time. Note that the measuring time of one time integral is one line frequency period T1, and double timeintegral requires 2T1. With more integral times, the precision of the measurement is higher but the measuring time is longer.

IX.CONCLUSION

This paper has presented an effective method to reduce the dc component in a three-phase transformerless grid-connected PV system. The dc component can introduce line-frequency power ripple in the system and further cause dc-link voltage ripple and second-order harmonics in the ac currents. A software-based “virtualcapacitor” approach has been implemented to minimize the dc component via a feed-forward of the dc component.Here fuzzy controller is used compared to alternative controllers because of its accurate performance.The Simpered Systems tool has demonstrated that the joint system will at the same time inject maximum power from a PV unit and compensate the harmonic current drained by nonlinear loads.The dc component can be accurately obtained using the descending window iteration and double time integral even under frequency variation and harmonic conditions. A PIR controller has been planned to allow the precise regulation of both the dc and line frequency components in the d-qframe.
The proposed method can be well adopted in the existing PV systems for dc component minimization by adding software programs for dc-component extraction, dc-component feed-forward term as well as the resonant controller in the current control loops.

ISSN(Online): 2319-8753
ISSN (Print): 2347-6710

International Journal of Innovative Research in Science, Engineering and Technology

(An ISO 3297: 2007 Certified Organization)

Website: www.ijirset.com

Vol. 6, Issue 8, August 2017

REFERENCES

[1] R. Gonzalez, E. Gubia, J. Lopez, and L. Marroyo, "Transformer less single-phase multilevel-based photovoltaic inverter,"IEEE Trans. Ind. Electron., vol. 55, no. 7, pp. 2694–2702, Jul. 2008.
[2] S. B. Kjaer, J. K. Pedersen, and F. Blaabjerg, "A review of single-phase grid-connected inverters for photovoltaic modules,"IEEE Trans.Ind. Appl., vol. 41, no. 5, pp. 1292–1306, Sep./Oct. 2005.
[3] E. Koutroulis and F. Blaabjerg, "Design optimization of transformerless grid-connected PV inverters including reliability,"IEEE Trans. PowerElectron., vol. 28, no. 1, pp. 325–335, Jan. 2013.
[4] B. Gu, J. Dominic, J. Lai, C. Chen, T. LaBella, and B. Chen, "High reliability and efficiency single-phase transformerlessinverter for grid-connected photovoltaic systems," IEEE Trans. Power Electron., vol. 28, no. 5, pp. 2235–2245, May 2013.
[5] S. V. Araujo, P. Zacharias, and R. Mallwitz, "Highly efficient single-phase transformerless inverters for grid-connectedphotovoltaic systems," IEEE Trans. Ind. Electron, vol. 57, no. 9, pp. 3188–3128, Sep. 2010.
[6] O. Lopez, F. D. Freijedo, A. G. Yepes, P. Fernandez-Comesaa, J. Malvar, R. Teodorescu, and J. Doval-Gandoy, "Eliminatingground current in a transformerless photovoltaic application," IEEE Trans. Energy Convers., vol. 25, no. 1, pp. 140–147,Mar. 2010.
[7] A. Ahfock and A. J. Hewitt, "DC magnetisation of transformers," IEEProc. Electro Power Appl., vol.153, no.4, pp. 601–607, Jul. 2006.
[8] B. Wang, X. Guo, H. Wu, Q. Mei, and W. Wu, "Real-time DC injection measurement technique for transformerless PVsystems," in Proc. IEEE2nd Int. Power Electron. Distribution Generation Syst., Hefei, China, Jun. 2010, pp. 980–983.
[9] W. Li, L. Liu, T. Zheng, G. Huang, and S. Hui, "Research on effects of transformer DC Bias on negative sequenceprotection," in Proc. Int.Conf. Adv. Power Syst. Automat. Protection, Beijing, China, Oct. 2011, pp. 1458–1463.
[10] A. Ahfock and A. J. Hewitt, "DC magnetisation of transformers," IEE Proc.-Electr Power Appl., vol. 153, no. 4, pp. 601–607, Jul. 2006.
[11] M. A. S. Masoum and P. S. Moses, "Impact of balanced and unbalanced direct current bias on harmonic distortion generated by asymmetric three-phase three-leg transformers,"IET Electr. Power Appl., vol. 4, no. 7, pp. 507–515, Jul. 2010.
[12] F. Berba, D. Atkinson, and M. Armstrong, "A review of minimization of output DC current component methods in single-phase grid-connected inverters PV applications," in Proc. 2nd Int. Symp. Environ. Friendly Energies Appl., Tyne, U.K., Jun. 2012, pp. 296–301.
[13] M. Armstrong, D. J. Atkinson, C. M. Johnson, and T. D. Abeyasekera, "Auto-calibrating DC link current sensing technique for transformerless, grid connected, H-bridge inverter systems,"IEEE Trans. Power Electron., vol. 21, no. 5, pp. 1385–1393, Sep. 2006.
[14] F. Berba, D. Atkinson, and M. Armstrong, "Minimization of DC current component in transformerless Grid-connected PV inverter application," in Proc. 10th Int. Conf. Environ.Elect. Eng., Rome, Italy, May 2011, pp. 1–4.
[15] Y. Shi, B. Liu, and S. Duan, "Eliminating DC current injection in current-transformer-sensed STATCOMs," IEEE Trans. Power Electron., vol. 28, no. 8, pp. 3760–3767, Aug. 2013.
[16] G. Buticchi, E. Lorenzani, and A. Fratta, "A new proposal to eliminate the DC current component at the point of common coupling for grid connected systems," inProc. IEEE 36th Ann. Conf. Ind. Electron. Soc., Glendale, USA, Nov. 2010, pp. 3244–3249.
[17] T.-F. Wu, H.-S. Nien, H.-M. Hsieh, and C.-L. Shen, "PV power injec-tion and active power filtering with amplitude-clamping and amplitude-scaling algorithms,"IEEE Trans. Ind. Appl., vol. 43, no. 3, pp. 731–741, May/Jun. 2007

BIOGRAPHY

B.LEELA PRIYAMVADA has graduated her B.Tech from Gowthami Institute of Technology & Management for Women, Proddatur, A.P., India. Currently she is pursuing M.Tech (EPS) from Sri Krishnadevaraya University College of Engineering and Technology, Ananthapuramu-515003, A.P., India. Her areas of interest are Electrical Power Systems.

Mr.V.K.CHAKRAVARTHI NAIK has received B.Tech degree from Sri Venkateswara University, Tirupathi. He received Master of Technology degree from G.Pullareddy Engineering College, Kurnool. Currently he is working as lecturer in the Department of Electrical and Electronics Engineering in Sri Krishnadevaraya University College of Engineering and Technology, Ananthapuramu-515003, Andhra Pradesh, India. His area of interest are Electrical Power Systems and Reliability.